JOURNAL OF SOLID STATE CHEMISTRY 27, 307–315 (1979)

The Electrical, Optical and Photoconducting Properties of $Fe_{2-x}Cr_xO_3$ ($0 \leq x \leq 0.47$)

P. MERCHANT, R. COLLINS, R. KERSHAW, K. DWIGHT AND A. WOLD*

Department of Chemistry, Brown University, Providence, Rhode Island 02912

Received May 11, 1978

A study has been made of the electrical, optical and photoconducting properties of pure and reduced single crystals of composition $Fe_{2-x}Cr_xO_3$ where $0 \leq x \leq 0.47$. It has been found that pure α-Fe_2O_3 is not a photoconductor. When defect-free crystals of α-Fe_2O_3 are reduced a surface layer of Fe_3O_4 is formed and the crystals exhibit photoconductivity. Removal of this layer resulted in the disappearance of photocurrents and an increase in the sample resistivity. A necessary condition for the observation of photocurrents in n-type Fe_2O_3 is that some Fe_3O_4 be present. In addition, it has been found that the substitution of chromium for iron in α-Fe_2O_3 results in a monotonically decreasing optical band gap as the chromium concentration, x, increases.

Introduction

Several reports (*1–5*) describing photoconductivity in n-type Fe_2O_3 have appeared in the literature. The interest in this material has been generated by its relatively narrow band gap (2.2 eV) (*1–5*) and its stability in aqueous solutions. However, it is apparent from these reports (*1–5*) that the composition of these samples, and therefore the origin of the observed photocurrents, is not well understood (see Table I). Even for the cases where analyses have been reported (*2, 3*), some questions remain concerning the composition of the products studied. In particular, the low resistivities listed in Table I are typical of the impure Fe_2O_3 samples previously characterized by Gardner *et al.* (*6*). It will be evident below that X-ray analysis, which was used to characterize the various products reported in Table I, is not as sensitive a technique as resistivity measurements in determining sample purity.

In this study, the electrical, optical and photoconducting properties of α–Fe_2O_3 have been measured on both pure and slightly reduced samples containing <1% Fe_3O_4. From these measurements the origins of the photocurrents previously reported in Fe_2O_3 samples can be determined. In addition, an investigation has been made to study the lowering of the optical band gap of α–Fe_2O_3 by making solid solutions of the system $Fe_{2-x}Cr_xO_3$. Since Cr_2O_3 has a band gap of 1.68 eV (*7*), members of this system should have band gaps between 1.68 eV and 2.2 eV.

Experimental

Members of the system $Fe_{2-x}Cr_xO_3$ were grown as large single crystal platelets (2–100 mm^2) by chemical vapor transport. Iron (III) oxide (Mapico Red), chromium (III) oxide (Jarrell–Ash) and approximately 20 mg of elemental tellurium were placed into 11 mm ID, 15 cm long silica tubes and

* To whom all correspondence should be addressed.

0022-4596/79/030307-09$02.00/0

TABLE I

PREPARATION AND ANALYSIS OF *n*-TYPE Fe_2O_3

Authors Ref. No.	Sample preparation	Structural and/or compositional analysis	ρ (300°K)	E_g (300°K)
Hardee and Bard (*1*)	Chemical vapor deposition (CVD) on Ti and Pt foils followed by firing to white-hot in Meeker burner flame for 1 min.	Polycrystalline from visual observation	"very low"	~2.14 eV from photocurrent onset
Quinn *et al.* (*2*)	Single crystals from PbF_2/PbO flux growth	Single crystal α-Fe_2O_3 from X-ray diffraction	500 Ω cm	~2.2 eV from photocurrent onset
Hardee and Bard (*3*)	CVD on Pt foil	Polycrystalline from CVD and salt evaporation. X-ray diffraction and SEM imply α-Fe_2O_3 with 20% ζ-Fe_2O_3, 10% γ-Fe_2O_3	Not reported	~2.2 eV from photocurrent onset
	Evaporation of Fe_2O_3 salts Natural Hematite	None		
Yeh and Hackerman (*4*)	Zone refined and magnetic iron and cold rolled steel heated red hot in air with Fisher burner for 15 min.	Polycrystalline from visual observation	Not reported	~1.4 eV from photocurrent onset
Kung *et al.* (*5*)	Hydrothermal growth of crystals with 8 M NaOH	Optical spectra suggests α-Fe_2O_3	<10 Ω cm	2.16 eV from optical density
This study	Chemical vapor transport using $TeCl_4$ as transport agent—Fe_2O_3 and $Fe_{2-x}Cr_xO_3$	X-ray diffractometer implies single phase α-Fe_2O_3 Cr content from neutron activation analysis	$>10^6$ Ω cm	2.16 ± 0.03 eV from optical density

evacuated to less than 2 torr. Chlorine gas was then introduced to give a partial pressure of 380 torr. The tubes were sealed and transport was attempted at several charge and growth zone temperatures. The conditions for successful transport, and the analyses of the products are given in Table II. The tubes were first heated in the back-transport mode for over 18 hr and then transport allowed to proceed for periods longer than 5 days. The samples were then removed from the tubes and washed in 3 M hydrochloric acid followed by rinsing with dilute ammonium hydroxide and finally by distilled water. The larger crystals showed a uniform blue-grey appearance by reflected light while the thinnest platelets were found to transmit red light, indicative of a band gap of approximately 2 eV.

Some of the pure Fe_2O_3 crystals were ground into powders and their composition analyzed using a Norelco x-ray diffractometer having a monochromatic, high intensity copper source [$\lambda(CuK\alpha_1) = 1.5405$ Å]. Slow scan patterns having silicon as an internal standard showed that these crystals were single phase α-Fe_2O_3 (corrundum structure) with lattice constants $a = 5.033$ Å, $c = 13.755$ Å. No evidence of the presence of Fe_3O_4 or other phases of Fe_2O_3

TABLE II

CONDITIONS FOR SUCCESSFUL GROWTH AND CHROMIUM ANALYSIS OF THE $Fe_{2-x}Cr_xO_3$ SINGLE CRYSTALS

Nominal composition	Back-transport time (hr)[a]	Transport time (hr)	Transport temperature gradient (°C)	Analysis[b]
Fe_2O_3	18	222	1000/900	α-Fe_2O_3
$Fe_{1.90}Cr_{0.10}O_3$	23	144	1075/900	$Fe_{1.91}Cr_{0.09}O_3$
$Fe_{1.80}Cr_{0.20}O_3$	23	144	1075/900	$Fe_{1.78}Cr_{0.22}O_3$
$FeCrO_3$	24	130	1000/900	$Fe_{1.79}Cr_{0.21}O_3$
$FeCrO_3$	23	238	1000/900	$Fe_{1.53}Cr_{0.47}O_3$

[a] In all cases the back-transport temperature gradient was 900/450°C.

[b] Analysis of the pure Fe_2O_3 sample was done by X-ray diffractometry. Chromium analysis was done by neutron activation analysis of the Cr^{51} ($\gamma = 321$ keV) peak.

was found in any of these crystals. Laue back-reflection photographs, taken with a General Electric XRD-3 diffractometer unit having a tungsten source showed that the $Fe_{2-x}Cr_xO_3$ platelets were oriented with their c-axes perpendicular to the large faces. The values of x in $Fe_{2-x}Cr_xO_3$ were determined by neutron activation analysis (see Table II).

The reduced samples were prepared by placing the crystals in evacuated silica tubes containing titanium turnings (not in direct contact with the crystals) and heating them to temperatures ranging from 350–425°C for periods exceeding 150 hr. These temperatures were determined by the appearance of Fe_3O_4 in the X-ray patterns of the products obtained by reducing pure α-Fe_2O_3 powders (see Fig. 1) for more than 12 hr at 50°C intervals ranging from 150–600°C. Resistance measurements were used to determine the reduction times for single crystals as follows. One of the α–Fe_2O_3 crystals, having a resistance greater than $10^8\ \Omega$ before reduction, was reduced at 375° for 193 hrs and its resistance was found to decrease to 6.6 kΩ. Further reduction of this sample for another 127 hr lowered the resistance to 2.2 kΩ. Because of the small relative change in the resistance of this sample for the second reduction, 150 h was chosen as a minimum time for the reduction of the crystals of this study.

The resistivities (ρ) of the samples were measured in the c-plane using the Van der Pauw technique (*8*). Ohmic contacts were obtained by the ultrasonic soldering of indium directly to the platelet edges. Hall effect measurements were not attempted since the samples showed magnetic behavior.

The optical measurements were taken at room temperature with unpolarized light in the 2100-270 nm region using a Cary

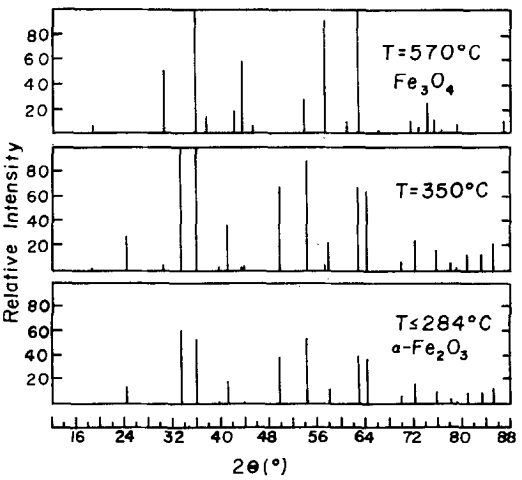

FIG. 1. X-ray powder diffraction patterns of α–Fe_2O_3 and Fe_3O_4. Note the appearance of Fe_3O_4 lines in the sample of α–Fe_2O_3 reduced at 350°C.

Model 17 spectrophotometer. Absorbance measurements were made with the light incident along the *c*-axis of the samples. The reflectivities of the samples were measured with the light incident at a 20° angle to the *c*-axis and ratioed against the calibrated reflectance of an evaporated aluminum film. None of the samples required polishing since the washed crystals had surfaces comparable to those obtained by polishing to a 0.05 μ finish.

The photoelectrolysis cell consisted of a platinized platinum cathode and semiconducting anode in a 0.2 M sodium acetate solution through which a 15% H_2, 85% Ar gas mixture was bubbled to purge the solution of dissolved oxygen. This gave a cathode potential of −0.65 volts with respect to the saturated calomel electrode (SCE). Illumination was provided by an Oriel 150 W xenon lamp which was focused into a 2 mm diameter spot (12.5 mW mm^2) at the anode. Measurements of the light and dark currents were taken at room temperature as a function of the bias voltage applied between the anode and cathode.

Results and Discussion

a. Pure Fe_2O_3

From Table I it is seen that the resistivity of the pure α-Fe_2O_3 samples exceeds 10^6 Ω cm. Such values of resistivity are characteristic of high purity α-Fe_2O_3 (*6*) (which exhibits intrinsic conductivity, since all of the iron present has the high spin state $3d^5$.)

Measurements of the optical density of thin platelets of pure α–Fe_2O_3 show the existence of a direct gap at 2.16±0.03 eV (see Fig. 2). This peak has been assigned to the $^6A_{1g} \rightarrow {}^4E_g\,(t_{2g})^3\,(e_g)^2$ crystal field transition by Tandon and Gupta (*9*). The lower energy peak at 1.44±0.03 eV has been assigned to the $^6A_{1g} \rightarrow {}^4T_{1g}\,(t_{2g})^4\,(e_g)$ crystal field transition by the same authors (*9*).

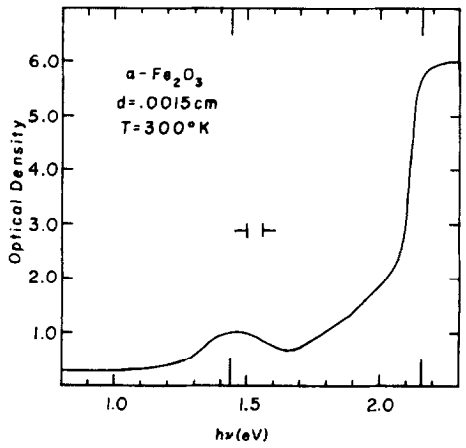

FIG. 2. The room temperature optical density of a 0.0015(5) cm thick platelet of α–Fe_2O_3 showing the crystal field transitions at 1.44(3) and 2.16(3) eV.

The large absorption coefficient of these samples for photon energies above 2.3 eV precluded transmission measurements. Consequently, reflectivity measurements were necessary to study the optical properties in this spectral region. In the UV there is a reflectance minimum at 3.64±0.04 eV (341 nm), as shown in Fig. 3. It may be of interest to note that the energy of this reflectance minimum coincides roughly with the energy of the peak in the photocurrent vs. photon energy curves for *n*-type Fe_2O_3 electrodes (*1–3*).

None of the pure α–Fe_2O_3 crystals showed any detectable change (≥5 μA cm^2) in their light vs. dark currents when placed in the

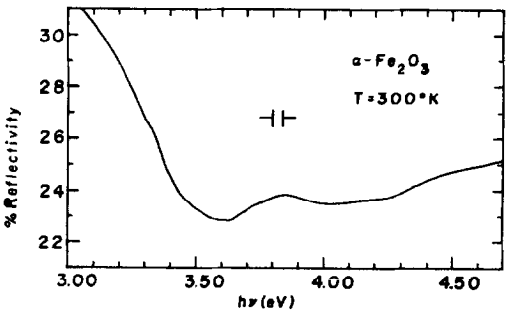

FIG. 3. The room temperature, unpolarized reflectivity of the *c*-face of an α–Fe_2O_3 crystal in the ultraviolet region of the spectrum.

photoelectrolysis cell. These results are consistent with the high purity and hence high resistivity of these crystals.

b. Reduced Fe_2O_3

It is well known that Fe_3O_4 (magnetite) is a good conductor at room temperature (*10*), having a band gap of 0.11 eV (*11*). Although the phase boundary between α–Fe_2O_3 and Fe_3O_4 is very sharp (*12*), α–Fe_2O_3 might be made conducting by the introduction of small amounts of Fe_3O_4 into the crystal by reduction. In this process, the removal of oxygen from the structure results in the separation of a spinel phase. Magnetite contains both Fe^{3+} and Fe^{2+} on octahedral sites, hence conduction can then occur via the transfer of electrons from Fe^{2+} to Fe^{3+}.

Upon removal of the reduced crystals from the reduction tubes, it was noticed that they had a blue-black, tarnished appearance in contrast to the blue-grey appearance of the pure α–Fe_2O_3 crystals. The results of the resistivity measurements are presented in Table III-a. It is interesting to note the constancy of the surface resistance (ρ/d) values with respect to reduction time and temperatures. In particular, all of the samples of group 3 were reduced in the same tube. Although their thicknesses and resistivities varied over about an order of magnitude, their surface resistances vary from one another by less than 20%. These results suggest that only a surface layer of conducting Fe_3O_4 is formed on the samples during reduction and hence that the resistivity of the bulk can be shorted by the surface layer.

A confirmation of this hypothesis was obtained by sanding the surfaces of four of the reduced samples and then measuring their resistivities again. The sanding was

TABLE III

RESISTIVITIES (300°K) OF THE REDUCED Fe_2O_3 SAMPLES

a. *Unpolished Samples*

Sample No.[a]	Reduction temperature (°C)	Reduction time (hr)	d (cm)	ρ (Ω cm)	$\rho/d(\Omega)$
1A	350	163	0.0020	1.7	850
1B	350	163	0.0046	3.7	800
2	375	320	0.0074	8.4	1150
3A	375	168	0.0030	3.1	1050
3B	375	168	0.0061	6.1	1000
3C	375	168	0.0097	8.0	800
3D	375	168	0.0150	16.4	1100
3E	375	168	0.0221	25.5	1150
4	400	160	0.0039	5.8	1500
5	400	167	0.0091	10.0	1100

b. *Polished Samples*

Sample No.	Reduction temperature (°C)	Reduction time (hr)	d (cm)	ρ (Ω cm)	$\rho/d(\Omega)$
1C	350	163	0.0084	2.2×10^4	2.6×10^6
3B	375	168	0.0060	53.0	8850
3C	375	168	0.0097	10.2	1050
3E	375	168	0.0210	97.0	4600

[a] Samples having the same number, i.e. 1A, 1B, 1C were reduced in the same tube.

accomplished by rubbing both faces and the outer edge with a dilute 600 grit emery paper for about 1 min under a pressure of a few ounces. The changes in thickness (d), resistivity (ρ), and surface resistance (ρ/d) of these samples, caused by the sanding process, can be seen from a comparison of Tables III-*a* and III-*b*. One of these samples, #1*c*, was sanded more heavily with 2/0 emery paper for about 2 min before being rubbed with the 600 grit paper. In this case, there was a nearly complete removal of the Fe_3O_4 layer as seen from its ρ and ρ/d values as well as from its return to a blue-grey appearance after sanding.

Samples 1A and 1B, which were not sanded, were ground into powders and X-ray diffractometer slow scans made for the appearance of the strongest Fe_3O_4 peaks. In both cases, no evidence of detectable amounts of Fe_3O_4 were found. However, as seen in Fig. 1, it is known that Fe_3O_4 is produced by reduction at temperatures greater than or equal to 350°C. It is therefore apparent that resistivity measurements are more sensitive than X-ray analysis in detecting small amounts of Fe_3O_4 in α–Fe_2O_3 crystals.

The optical densities of three of the reduced α–Fe_2O_3 samples were also measured in the 2100–550 nm region of the spectrum. While the positions of the absorption bands of these samples were identical to those found in the pure Fe_2O_3 samples, it was found that the overall absorbance in the measured spectral region had increased by a constant amount. Since the band gap of Fe_3O_4 occurs below the long-wavelength edge of the spectral region covered by these measurements, a surface layer of Fe_3O_4 should therefore contribute to an additional absorbance in these samples. The constancy of this extra absorbance is consistent with the fact that these measurements were taken at energies above the band gap of Fe_3O_4, where its absorption coefficient is nearly constant (*11*).

Photocurrent measurements were taken from several of the reduced α–Fe_2O_3 samples. Fig. 4 shows a plot of the light and dark currents of one of these samples (#1*c* from Table III-b, reduced at 350°C for 163 hr) as a function of the applied bias. Of interest is the lack of saturation of the photocurrent for the larger bias voltages. This effect was also seen in the other samples of this study as well as in the CVD films of Hardee and Bard (*1, 3*). After removal from the photoelectrolysis cell, this sample was sanded with 2/0 emery paper and its photocurrent measured again. No detectable photocurrents were found after this treatment.

The observation of photocurrents in reduced α–Fe_2O_3, but not in pure α–Fe_2O_3, implies that a necessary condition for the observation of photocurrents in Fe_2O_3 is that it contain mixed valency iron ions. An unfortunate aspect of the reduction of pure, defect free α–Fe_2O_3 crystals is that only a surface layer of Fe_3O_4 could be formed. As a result, the photocurrents of these samples are limited by the recombination of holes,

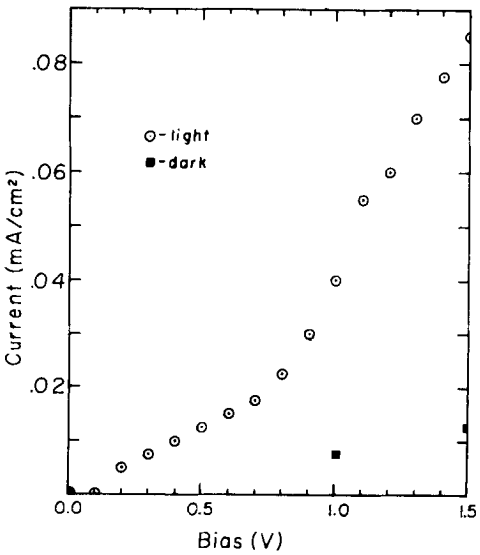

FIG. 4. Light and dark currents vs. applied bias for a defect-free α–Fe_2O_3 platelet reduced at 350°C for 163 hr (before sanding), in oxygen-free 0.2 M sodium acetate with the cathode at −0.65 volts vs. SCE.

migrating toward the anode–electrolyte interface, with mobile electrons in the conducting surface layer. Attempts to convert a large part of the pure Fe_2O_3 crystals to Fe_3O_4 resulted in the collapse of the crystal structure. This is due to the inability of the corundum structure to tolerate large concentrations of spinel inclusions.

However, some of the α–Fe_2O_3 crystals were found to have terraced faces, indicative of uneven growth rates in different regions of the crystals. It is well known that in such crystals there exist dislocation networks forming grain boundaries (*13*). A reduction of these defect crystals might result in the formation of Fe_3O_4 along dislocations where the structure can accommodate spinel inclusions more readily than in more perfect regions of the crystal, thus providing a more uniform mixture of Fe_2O_3 and Fe_3O_4 than in the reduced, defect free platelets.

The results of several photocurrent measurements on one of the reduced defect crystals are presented in Fig. 5. The data for

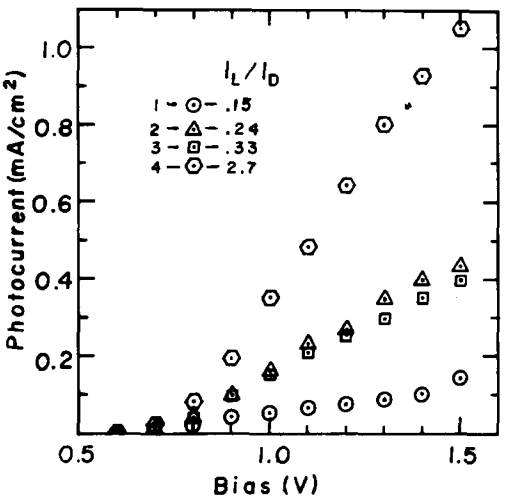

FIG. 5. Photocurrents vs applied bias for a defect crystal of α–Fe_2O_3 reduced at 350°C for 218 hr, in oxygen-free 0.2 M sodium acetate with the cathode at −0.64 volts vs SCE. The initial behavior and that after successive stages of sanding are shown in curves 1–4, respectively. The corresponding values for the ratios of light to dark currents at 1.5 V bias are given with the plotting symbols.

curve 1 was taken when this sample was first placed in the photoelectrolysis cell. Upon removal from the cell, its surface was lightly sanded with 2/0 emery paper for about 2 min followed by a similar abrasion with dilute 600 grit emergy paper. It was then replaced in the cell and the points of curve 2 measured. Further repetition of the sanding process resulted in the curves labeled 3 and 4, respectively. It is evident from these plots that there is a large increase in the photocurrent as the conducting surface layer of Fe_3O_4 is removed. As seen from the insert of Fig. 5, the removal of the survace layer is coupled with an increase in the photocurrent to dark current ratio (I_l/I_d). Further sanding of this sample did not result in any significant changes from the results of curve 4. It is therefore apparent that curve 4 is indicative of the photoconducting behavior of the bulk of this sample.

These results can be interpreted in the following manner. The photocurrents of the unsanded sample (curve 1) are limited by recombination in the conducting Fe_3O_4 surface layer. This view is supported by the relatively large dark currents of this sample before sanding. As the conducting surface layer is removed, the dark currents decrease and the photocurrent increases because of the more homogeneous distribution of Fe_3O_4 in α–Fe_2O_3 below the surface. When the surface layer is completely removed, as for curve 4, the true photoconductivity of the bulk is evident.

c. $Fe_{2-x}Cr_xO_3$, $x \neq 0$

The effect of Cr doping on the band gap of α–Fe_2O_3 is presented in Fig. 6 for $0 \leq x \leq 0.47$. For the range of compositions studied, it is apparent that there is a monotonic decrease in the gap of this material as the chromium content, x, increases. The nature of this shift of the energy gap with chromium content can be clarified with a comparison of the optical densities of pure and chromium-doped Fe_2O_3, shown in Fig. 7. It is apparent

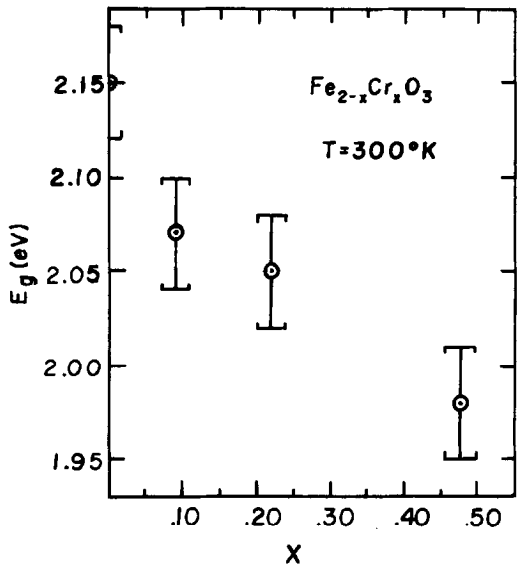

FIG. 6. The dependence of the optical band gap of $Fe_{2-x}Cr_xO_3$ vs. chromium content (x), at room temperature.

that the 1.44 eV transition in α–Fe_2O_3 has been shifted to higher energies, whereas the band gap transition is shifted to lower energies, consistent with a reduction in the crystal field splitting of the $t_{2g}-e_g$ levels when chromium is substituted for iron in these samples.

The resistivities of the $Fe_{2-x}Cr_xO_3$ samples listed in Table II were also measured. For all of these samples, the resistivities remained larger than $10^6\ \Omega$ cm at room temperature. This result is interesting since, in these crystals, the chromium ions are stable in the +3 valence state, $3d^6$. Although the impurity concentration is large, the crystals are not conducting since the iron is still present in only the +3 valence state.

Some of the $Fe_{2-x}Cr_xO_3$ crystals were reduced under conditions similar to those used to reduce the pure α–Fe_2O_3 samples. However, the reduced products possessed no mechanical strength, and fell apart during attempts to attach leads.

Finally, photocurrent measurements were attempted on some of the unreduced $Fe_{2-x}Cr_xO_3$ samples. The lack of mixed valency iron and hence the high resistivity of these samples resulted in no detectable photocurrents in any of these samples.

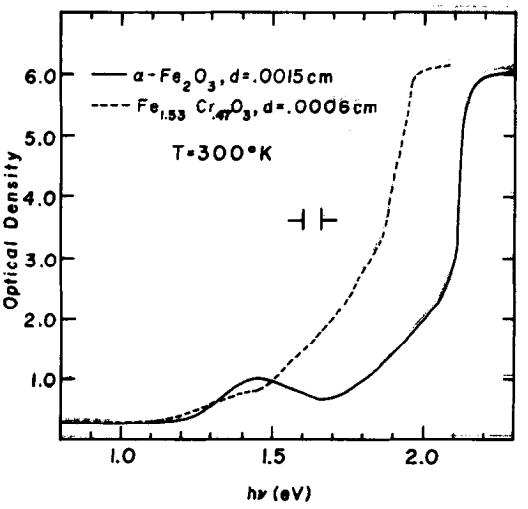

FIG. 7. The room temperature optical densities of α–Fe_2O_3 (solid curve) and $Fe_{1.53}Cr_{0.47}O_3$ (dashed curve) showing the shift in the crystal field splitting of the 3d levels with chromium substitution.

Conclusions

Several conclusions may be drawn from the results presented above. First, pure α–Fe_2O_3 is not a photoconductor because of its high resistivity which results from the presence of iron in only a single valence state. A necessary condition for the observation of photocurrents in α–Fe_2O_3 is that it contain Fe^{2+} and Fe^{3+}. When pure, defect free crystals of α–Fe_2O_3 are reduced, only a surface layer of conducting Fe_3O_4 is formed. While this surface layer is responsible for photoconductivity in these crystals, its removal results in a disappearance of the photocurrents in these samples. When crystals containing dislocations are reduced, Fe_3O_4 can form both on the surface and along the dislocations. In this case, the photocurrents increase when the surface layer is removed

since this layer reduces the photocurrents by recombination. Therefore, it is desirable to have a homogeneous mixture of Fe^{2+} and Fe^{3+} present in the crystals to minimize recombination losses. Finally, one can lower the band gap of α–Fe_2O_3 by the formation of the solid solution $Fe_{2-x}Cr_xO_3$.

Acknowledgments

The Office of Naval Research, Arlington, Virginia supported the work of Paul Merchant and Kirby Dwight. Acknowledgement is made to the Donors of the Petroleum Research Fund, administered by the American Chemical Society, Washington, D.C. for support of R. Collins. In addition, the authors would like to acknowledge the support of the Materials Research Laboratory Program at Brown University.

The authors wish to express their appreciation to Dr. S. N. Subbarao for his assistance in the study of photocurrents, to Dr. M. Doyle of the State of Rhode Island Nuclear Reactor Facility for assistance in all aspects of the neutron activation analysis, and Professor C. Elbaum of the Brown University Physics Department for several helpful discussions.

References

1. K. L. HARDEE AND A. J. BARD, *J. Electrochem. Soc.* **123**, 1024 (1976).
2. R. K. QUINN, R. D. NASBY, AND R. J. BAUGHMAN, *Mater. Res. Bull.* **11**, 1011 (1976).
3. K. L. HARDEE AND A. J. BARD, *J. Electrochem. Soc.* **124**, 215 (1977).
4. L. R. YEH AND N. HACKERMAN, *J. Electrochem. Soc.* **124**, 833 (1977).
5. H. H. KUNG, H. S. JARRETT, A. W. SLEIGHT, AND A. FERRENTTI, *J. Appl. Phys.* **48**, 2463 (1977).
6. R. F. G. GARDNER, F. SWEETT, AND D. W. TANNER, *J. Phys. Chem. Solids* **24**, 1175 (1963); *ibid*, **24**, 1183 (1963).
7. J. A. CRAWFORD AND R. W. VEST, *J. Appl. Phys.* **35**, 2413 (1964).
8. L. J. VAN DER PAUW, *Phillips Res. Rep.* **13**, 9 (1958).
9. S. P. TANDON AND J. P. GUPTA, *Spectrosc. Lett.* **3**, 297 (1970).
10. A. J. M. KUIPERS AND V. A. M. BRABERS, *Phys. Rev., B* **14**, 1401 (1976).
11. U. BUCHENAU AND I. MÜLLER, *Solid State Commun.* **11**, 1291 (1972).
12. O. N. SALMON, *J. Phys. Chem.* **65**, 550 (1961).
13. W. T. READ, JR., "Dislocations in Crystals," McGraw-Hill, New York (1953).